4B1-3

Localization of living-bodies using single-frequency MIMO radar system

#Takashi Miwa, Yasuto Kigure, Yoshiki Yamakoshi
Department of Electronic Engineering, Gunma University
1-5-1 Tenjin-cho,Kiryu-shi, Gunma, 376-8515 Japan
miwa@el.gunma-u.ac.jp

1. Introduction

Recently, huge earthquakes, landslide and flood disasters have frequently happened all around the world. In order to prevent victims increasing, it is one of the most important problems to localize the 3D position of the survivor buried under the collapsed house, rubble and soil as soon as possible. Many living-body detection systems have already been developed which are based on the monostatic pulsed Doppler radar system [1]. Because the displacement of the breast motion is about 1 cm by breathing, the frequency range around GHz is used. Thus, the measurement area is limited. If we apply a bistatic MIMO radar technology to this system, we would quickly estimate the 3D position in the wide area. However, to widen measurement area increases the signal attenuation by propagating the medium. So, we develop a single frequency MIMO Doppler radar system around 250 MHz. We discuss the localization algorithm based on beamformer algorithm by using the complex amplitude at the Doppler frequency measured with MIMO radar and apply MUSIC algorithm to improve the resolution [2][3].

2. Outline of MIMO radar system

Figure 1 shows the block diagram of developed single-frequency MIMO radar system. This system can measure the matrix transfer function between 8 transmitting and 8 receiving antennas from 200 to 350 MHz. The phase lock loop (PLL) circuit generates a single local frequency (512 MHz) using a reference signal (19.2 MHz) led from TCXO. A directional coupler distributes a transmitting signal into a local signal for receiver. The frequency of the transmitting signal is divided by 256 MHz at a 1/2 pre-scaler circuit and amplified with a power amplifier up to 15 dBm. The SP8T switch IC sequentially switches the transmitting signal for 8 antennas through coaxial cables. The return loss and isolation of the switches is measured by 30 dB and 35 dB, respectively. The power of the local signal is divided by resistor-based power divider and led to 8 IQ detectors as a local signal. We use a quadrature demodulator (AD8348) as a IQ detector. This IC needs a local signal having twice the frequency of a RF signals because of generating a quadrature signals internally. Each IQ detector detects a IQ signal of the transfer function obtained in each receiver. The IQ signals are measured by 16 channel-16 bit A/D converter board having a sampling frequency of up to 100 kHz / 1 channel. So, IQ signals of 8 receivers are obtained with the sampling frequency of 6.25 kHz. The switching frequency of transmitter is 781Hz, which is almost same as cut off frequency of baseband lowpass filter of IQ detectors by considering the transient response due to transmitting switch. Therefore, the total sampling frequency is 97.7 Hz to obtain 8*8 matrix transfer functions. This system has a dynamic range of 100 dB for 0.3 Hz in the case of 90 seconds sampling.

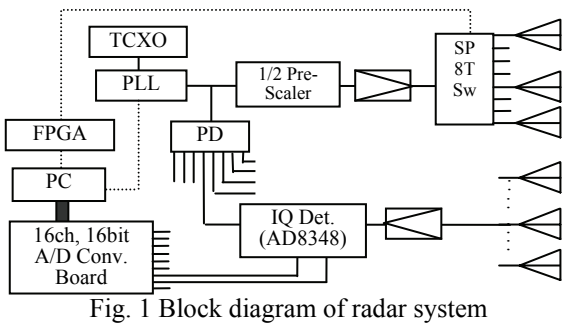

Fig. 1 Block diagram of radar system

ISBN: 978-4-88552-223-9 C3055©IEICE

3. Imaging algorithm

3.1 Analysis model

Figure 2 shows a system model to be considered in this analysis. The small electric dipole antennas are assumed as transmitters and receivers in this system and are arraigned at arbitrarily position and orientation. A target is modelized as a sphere having much smaller radius than the wavelength. The radius is time-dependently changed as $a(t) = a_0 + \Delta a(t)$. $\boldsymbol{i}_r$ and $\boldsymbol{i}_p$ are a unit vector oriented to incidence and polarization, respectively, in a spherical co-ordinate. Also, $\boldsymbol{i}_x$ is defined as a unit vector perpendicular to $\boldsymbol{i}_r$ and $\boldsymbol{i}_p$. Here, $\theta^s_{i,j,k}$ is an angle between $\boldsymbol{i}_r$ and scattered orientation. Also $\varphi^s_{i,j,k}$ is defined as an angle between $\boldsymbol{i}_x$ and the orientation to which the scattered orientation is projected onto the plane including $\boldsymbol{i}_p$ and $\boldsymbol{i}_x$. Generally, the scattered wave from the target is expressed as $S(\theta^s, \varphi^s, a(t), \beta_0, r)$. If $\Delta a(t)$ is much smaller than the wavelength, the following approximation holds:

$$S(\theta^s, \varphi^s, a(t), \beta_0, r) \approx S(\theta^s, \varphi^s, a_0, \beta_0, r)\exp(j\beta_0 \Delta a(t)) \tag{1}$$

Eq. (1) means that the change of the directivity depends on only the phase change by the motion of target radius. Moreover, if we consider that θ^s and φ^s can be limited in the limited area, the following second approximation holds:

$$S(\theta^s, \varphi^s, a_0, \beta_0, r) \approx \Gamma(a_0, \beta_0)\exp(-j\beta_0 r)/r \tag{2}$$

Eq. (2) means that the scattering signal is a function of the distance between receivers and scatterers.

On the other hand, $\theta^t_{i,k}$ and $\theta^r_{j,k}$ is a transmitting and incidence angle of the antenna. The scattered wave vector $\boldsymbol{p}_k$ and $\boldsymbol{q}_k$ obtained in each transmitting and receiving antenna are expressed with a spherical mode vector whose elements have $p_{i,k}$ and $q_{j,k}$.

$$p_{i,k} = \frac{\sin(\theta^t_{i,k})}{l^t_{i,k}}\exp(-j\beta_0 l^t_{i,k}) \qquad q_{j,k} = \frac{\sin(\theta^r_{j,k})}{l^r_{j,k}}\exp(-j\beta_0 l^r_{j,k}) \tag{3}$$

Here, the matrix transfer function between each transmitter and each receiver obtained from D scatterers is expressed as follows:

$$\begin{aligned} \boldsymbol{X}_s(t) &= A\sum_{k=1}^{D} \boldsymbol{q}_k \Gamma_k \boldsymbol{p}_k^{\mathrm{T}} \exp(j\beta_0 \Delta a(t)) \\ &= A\boldsymbol{Q}\cdot\boldsymbol{\Gamma}\cdot\boldsymbol{P}^{\mathrm{T}}\exp(j\beta_0\Delta a(t)) \end{aligned} \tag{4}$$

$$\begin{aligned} \boldsymbol{Q} &= [\boldsymbol{q}_1 \quad \boldsymbol{q}_2 \quad \cdots \quad \boldsymbol{q}_D] \\ \boldsymbol{P} &= [\boldsymbol{p}_1 \quad \boldsymbol{p}_2 \quad \cdots \quad \boldsymbol{p}_D] \\ \boldsymbol{\Gamma} &= \mathrm{diag}(\Gamma_1 \quad \Gamma_2 \quad \cdots \quad \Gamma_D) \end{aligned} \tag{5}$$

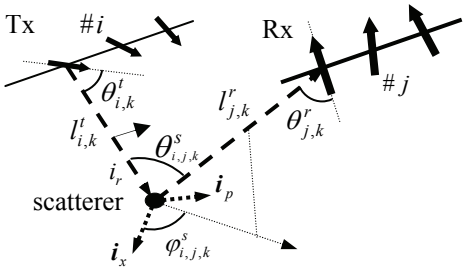

Fig.2 Definition of the antenna array and target

Where A, D and T means multiplication of the antenna effective length, number of the scatterers and transpose of the matrix, respectively. Here, the received signals $\boldsymbol{X}(t)$ is expressed as follows by using the signal scattered from stationary targets $\boldsymbol{X}_d$ and noise signal $\boldsymbol{X}_N(t)$:

$$\boldsymbol{X}(t) = \boldsymbol{X}_d + \boldsymbol{X}_s(t) + \boldsymbol{X}_N(t) \tag{6}$$

Here, we assume that $\boldsymbol{X}_s(t)$ periodically varies with the frequency of f_a. The Fourier transformation of each element of $\boldsymbol{X}(t)$ can reject the signal from the stationary targets as follows:

$$\boldsymbol{Y}(f_a) = A\boldsymbol{Q}\cdot\boldsymbol{\Gamma}\cdot\boldsymbol{P}^{\mathrm{T}}C(f_a) + \boldsymbol{Y}_N(f_a) \tag{7}$$

Where $C(f_a)$ is a Fourier coefficient of $\exp(j\beta_0\Delta a(t))$ at frequency f_a, which is generally expressed as a Bessel function. Therefore, $\boldsymbol{Y}(f_a)$ keeps the information of the position of the targets even if the Fourier transformation is applied.

3.2 MIMO-Beamformer algorithm

To estimate the 3D position of the target, we use conventional space-steering algorithm. Here, we define the receiving and transmitting steering vector $\boldsymbol{v}_r(x,y,z)$ and $\boldsymbol{v}_t(x,y,z)$ as a

spherical mode vector whose elements have $q_{j,k}$ and $p_{i,k}$ for the target position (x,y,z) ,respectively. The beamformer algorithm is based on searching the maximum correlated position between the received signal matrix and steering vector. Thus, the following evaluation function can be defined:

$$P_B = \left| \boldsymbol{v}_r(x,y,z)^H \boldsymbol{Y}(f_a) \boldsymbol{v}_t(x,y,z)^* \right|^2 \Big/ \left| \boldsymbol{v}_r(x,y,z) \right|^2 \left| \boldsymbol{v}_t(x,y,z) \right|^2 \quad (8)$$

Where H and * means complex conjugate transpose and complex conjugate.

3.3 MIMO-Music

The correlation matrix of the received signal $\boldsymbol{R}_{YY} = \mathrm{E}[\boldsymbol{Y}(f_a)\boldsymbol{Y}(f_a)^{\mathrm{H}}]$ is expressed as follows:

$$\boldsymbol{R}_{YY} \approx \boldsymbol{Q}\Gamma\boldsymbol{P}^{\mathrm{T}}\boldsymbol{P}^*\Gamma^*\boldsymbol{Q}^{\mathrm{H}} + \sigma\boldsymbol{I} \quad (9)$$

The eigen-analysis of Eq.(9) can separate the signal eigenspace and the noise eigenspace by comparing the eigenvalues to the noise variance. When the number of antennas is *N*, we can obtain the *N-D* noise eigenvector $\boldsymbol{e}_m$ (m=1,2,..*N-D*). Thus, the following MUSIC spectrum obtained from receiving array is obtained:

$$P_r(x,y,z) = \frac{\left| \boldsymbol{v}_r(x,y,z) \right|^2}{\sum_{m=1}^{N-D} \left| \boldsymbol{e}_m^{\mathrm{H}} \boldsymbol{v}_r(x,y,z) \right|^2} \quad (10)$$

The transpose of $\boldsymbol{Y}$ means the receiving matrix when the transmitter and receiver are exchanged each other. So, we can obtain the MUSIC spectrum $P_t(x,y,z)$ from the transmitter side by using $\boldsymbol{Y}^{\mathrm{T}}$, then MUSIC spectrum P_M is expressed as follows

$$P_M(x,y,z) = \frac{P_r(x,y,z)P_t(x,y,z)}{P_r(x,y,z) + P_t(x,y,z)} \quad (11)$$

4. Experimental results

To demonstrate the validity of the MIMO radar system and to estimate the position of living body, the experiment was carried out at the open site. Figure 3 shows the overview of the experimental site. The linear transmitting and receiving array have the number of element of 8, the antenna separation of 0.58 m (half wavelength), the array aperture of 4.06 m and the array separation of 7.6 m. The array height is 1.9 m. The half wavelength dipole antennas with balun are used. The antennas are arraigned co-linearly to the array axis because the change of the antenna directivity reduces. Figure 4(a) shows the measured IQ signal for 84sec when the target is a living body lying on the ground. We can see the phase difference caused by the vibration of the breast in both the IQ signals. Figure 4(b) shows the measured power spectrum obtained by Fourier transformation of the measured IQ signals in blue line. We can find a clear Doppler spectrum peak around 0.25 Hz caused by the breast motion of the target. In this range, the dominant noise source is not white noise but phase noise

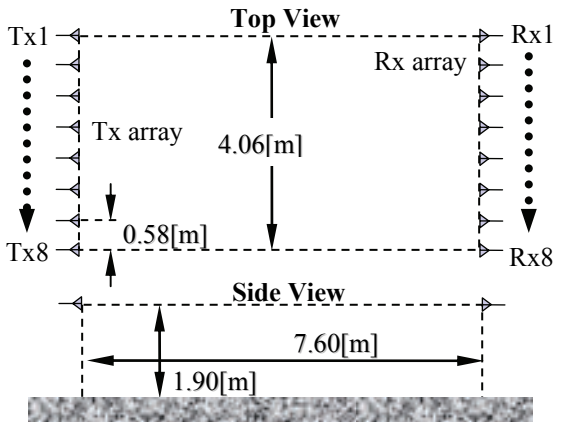

Fig. 3 Overview of the experimental site

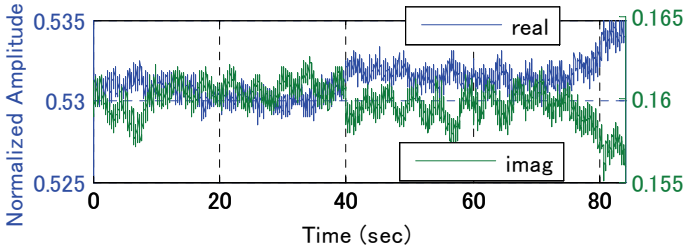

(a) Measured IQ signal

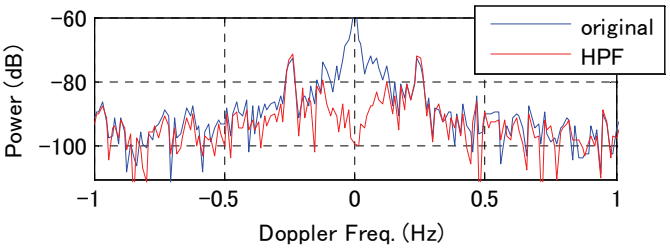

(b) Power spectrum

Fig. 4 Example of received signal for 82sec. sampling

generated by the crystal oscillator. The S/N ratio is estimated to be about 10 dB for a single channel. The red line shows the power spectrum after applying subtraction of the moving average for 5sec.

Figure 5 shows the estimation result of the position of the target. Fig.5 (a) and (b) correspond to the beamformer and MUSIC result, respectively. The symbol +, x and o means the position of the transmitter, receiver and target, respectively. The maximum value of P_B appears at the breast of the living body in Fig.5 (a). This means that the complex amplitude extracted at the Doppler frequency has the information of the target position. But, it is found that the resolution in the y direction is much lower than that in the x direction. Because the spherical mode vector approaches the plane wave mode vector as the propagation distance from the array increases. On the other hand, it is observed that the resolution of y direction is improved in Fig.5 (b) by MUSIC algorithm. Figure 6 shows imaging results for both a human and a metallic hemisphere having the diameter of 40 cm. The reflector can sinusoidally vibrate with the displacement of 7 mm by the electromagnetic shaker. Even if the number of the target is increased, the peaks of the image appear around the true target position.

5. Conclusion

In this paper, we presented a developed MIMO radar system to estimate the position of living bodies. This system has a sufficient SNR to detect the target position in free space. We showed the complex amplitude of the Doppler peak obtained in each channel has information of the position of the target in the frequency range of 256 MHz. It is also shown that the MUSIC algorithm is applicable to localization of the target with this system. It is a future work to analyze the optimal antenna arrangement and to evaluate the resolution and accuracy in much more realistic situation.

Acknowledgments

This work is partially supported by grant-in-aid for scientific research-18760301. A part of this work has been performed at the Venture Business Laboratory in Gunma University.

References

[1] K. Chen, etc, ”Microwave life-detection system for searching human subjects under earthquake rubble or behind barrier,” *IEEE Trans. Biome. Eng.*, vol. BME-47, no. 1, pp. 105-114, Jan. 2000.

[2] T. Miwa and I. Arai, “Super-resolution imaging for point reflectors near transmitting and receiving array,” *IEEE Trans. Antennas and Propagat.*, vol. 52, no. 1, pp. 220-229, Jan. 2004.

[3] S. K. Lehman and A. J. Devaney, “Transmission mode time-reversal super-resolution imaging”, *The journal of Acous. Soc. of Am.*, vol. 13, No.5, pp.2742-2753, May 2003.

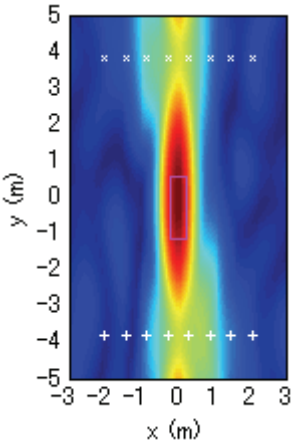

(a) Beamformer algorithm

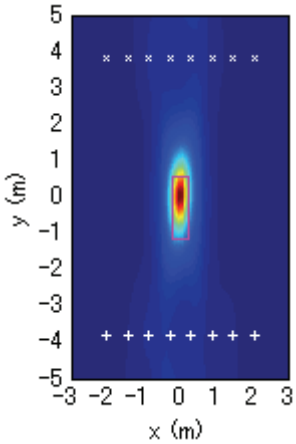

(b) MUSIC algorithm

Fig. 5 Imaging result for breathing living body

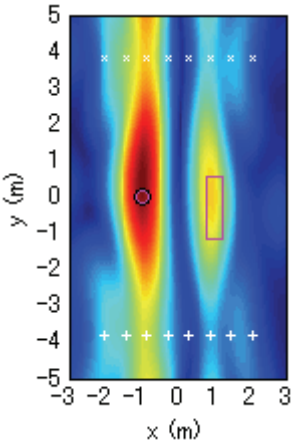

(a) Beamformer algorithm

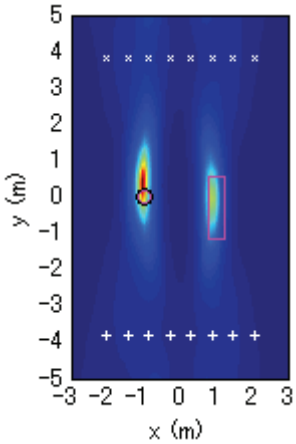

(b) MUSIC algorithm

Fig. 6 Imaging result for vibrated target and human